DYNAMICS OF MAGNETIC HOLES IN A ROTATING FIELD

by

Piotr Pierañski[+], Arne Skjeltorp[++] and Riccardo Barberi[+++]

-

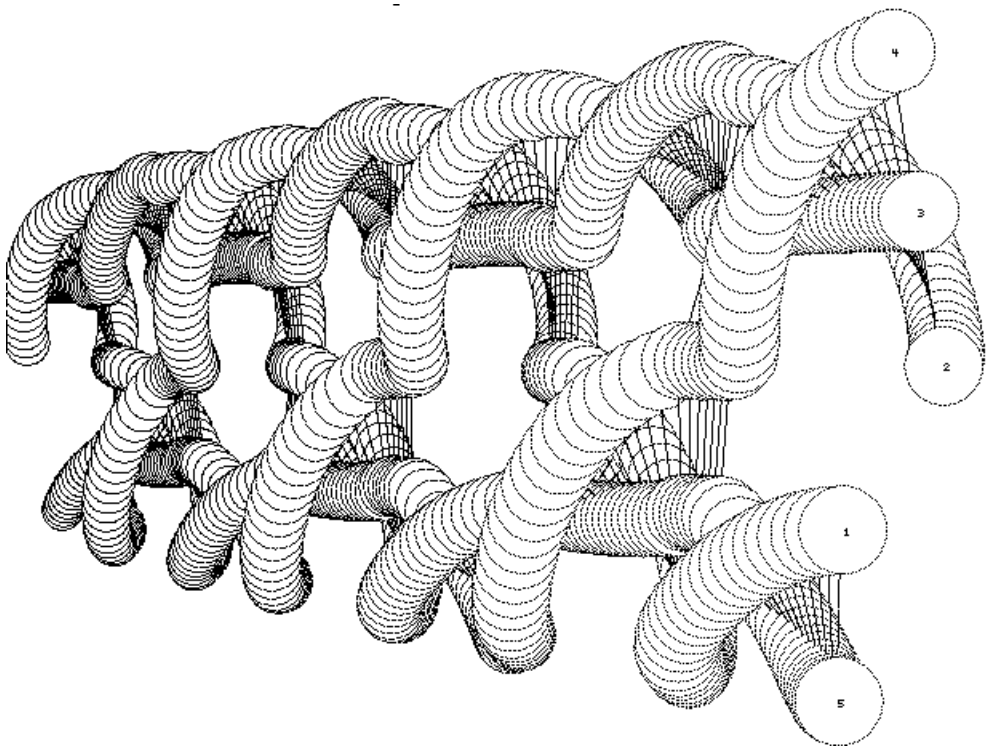

+ Institute of Molecular Physics, Smoluchowskiego 17/19, 60 179 Poznañ, Poland

++ Institute for Energy Technology, 2007 Kjeller, Norway

+++University of Calabria, Department of Physics, 87 036 Arcavacata di Rende, Italy

INTRODUCTION

Magnetic hole is a bubble in a magnetised ferrofluid.[1] When a non magnetic solid particle is submerged within a ferrofluid, a stable, fixed volume and shape magnetic hole is formed. Highly monodisperse, almost perfectly spherical, magnetic holes are easily obtained when polystyrene microspheres are mixed with a ferrofluid. (In what follows terms *magnetic hole* and *sphere* mean the same.)

Magnetic holes interact via dipolar forces. Each magnetic hole carries a magnetic dipole moment of a magnitude equal to the magnetisation of the ferrofluid it replaces and oriented in the opposite direction. When a ferrofluid sample containing monodisperse microspheres is placed in a uniform magnetic field $\vec{H}$, all magnetic dipoles carried by the spheres are equal in their magnitudes and parallel to each other:

$$\vec{\mu} = -V\chi_{eff}\vec{H}, \qquad (1)$$

where V is the volume of a microsphere and χ_{eff} is the effective volume susceptibility of the ferrofluid.

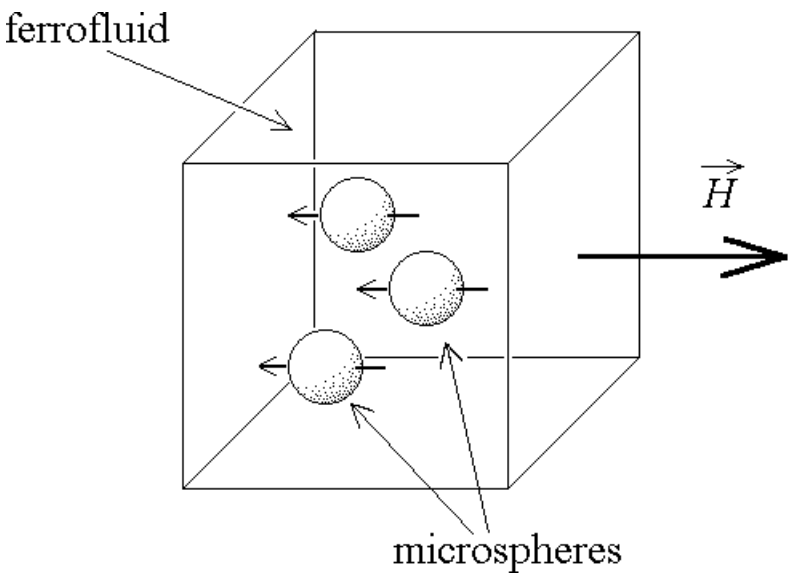

Fig.1 Plastic microspheres submerged in a magnetised ferrofluid - a practical realisation of the idea of magnetic holes.

That all dipole moments are parallel to each other, simplifies considerably their interactions. The total interaction energy of *N* magnetic holes is given by:

$$U(\vec{r}_1,\vec{r}_2,...,\vec{r}_N,t)=\sum_{i=1}^{N}\sum_{j=i+1}^{N}\left\{\frac{\mu^2(t)}{r_{ij}^3}-\frac{3\left[\vec{\mu}(t)\cdot\vec{r}_{ij}\right]^2}{r_{ij}^5}\right\} \qquad (2)$$

where $\vec{r}_{ij}=\vec{r}_j-\vec{r}_i$ is the vector joining centres of the interacting spheres.

For a time dependent (e.g. rotating) magnetic field the dipole moments are also time dependent, what is *explicite* marked in the equation. One must remember, however, that as long as the time dependent magnetic field stays uniform, the magnetic dipole moments carried by each of the holes stay parallel to each other and Eq.2 preserves its validity.

EXPERIMENTAL SET-UP

Experiments we performed were carried out in a planar geometry. The ferrofluid with polystyrene microspheres dispersed in it was contained in a thin box formed by two parallel glass plates (microscope slide and cover glass). The distance between the plates was typically twice the diameter σ of the microspheres, where σ was about 100 μm. The cell was placed within a system of two pairs of coils producing magnetic field rotating within the plane of the cell. A transmission optical microscope was used to observe motion of the microspheres. See Fig.2. Interesting modes of motion were recorded using a video-tape recorder.

The number N of microspheres in the central part of the sample (seen within the view field of the microscope) was controlled by means of a hand-held magnet, which allowed the experimenter to push away unwanted spheres, or pull the wanted ones into the view.

Experiments with N=2,3,...,10 spheres were performed with the aim to determine typical modes of their motion at various frequencies of the rotating field. In

what follows we shall describe results of numerical simulations of such experiments. As indicated in Fig.2, motion of the microspheres was limited to the (x, y)-plane. In the experiments we shall describe, vector of the magnetic field was also limited to the plane. Thus, the whole problem becomes two-dimensional.

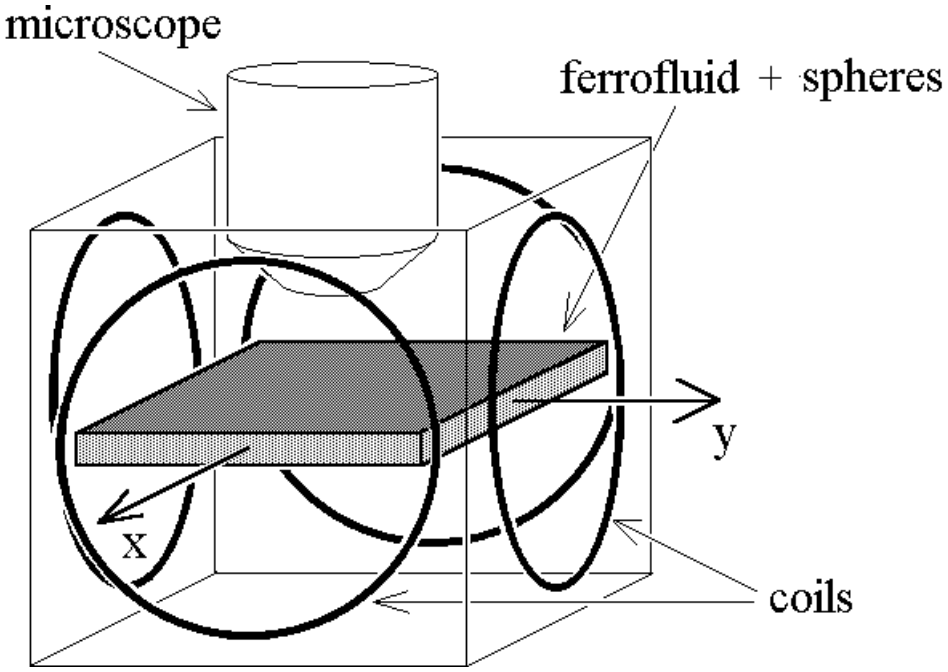

Fig. 2 Experimental set-up.

Numerical simulations we present below are carried out in the same planar geometry.

EQUATIONS OF MOTION AND THE NUMERICAL SIMULATION PROCEDURE

Starting from Eq.2 one can easily find magnetic forces acting on each of the spheres. For reasons explained above, only the x and y components of the forces are relevant here. As easy to find, the force on i-th sphere is described by the following equations:

$$F_{i,x} = -\sum_{j\neq i}\frac{\partial}{\partial x_j}U(\vec{r}_1,\vec{r}_2,,...,\vec{r}_n) = \\ = \sum_{j\neq i}\left\{-3\frac{\mu^2(x_j-x_i)}{r_{ij}^5}+15\frac{(x_j-x_i)(\vec{\mu}\cdot\vec{r}_{ij})^2}{r_{ij}^7}-6\frac{\mu_x(\vec{\mu}\cdot\vec{r}_{ij})}{r_{ij}^5}\right\} \tag{3}$$

$$F_{i,y} = -\sum_{j\neq i}\frac{\partial}{\partial y_j}U(\vec{r}_1,\vec{r}_2,,...,\vec{r}_n) = \\ = \sum_{j\neq i}\left\{-3\frac{\mu^2(y_j-y_i)}{r_{ij}^5}+15\frac{(y_j-y_i)(\vec{\mu}\cdot\vec{r}_{ij})^2}{r_{ij}^7}-6\frac{\mu_y(\vec{\mu}\cdot\vec{r}_{ij})}{r_{ij}^5}\right\} \tag{4}$$

where for the field $\vec{H}(t)$ rotating with angular velocity ω all magnetic dipole moments carried by the spheres are described by:

$$\mu_x(t) = \alpha H_x \sin(\omega t) \\ \mu_y(t) = \alpha H_y \cos(\omega t) \tag{5}$$

For all considered below cases we assumed that $H_x=H_y=H$.

In view of the large viscosity of the ferrofluid inertial forces can be neglected. Thus, we assumed that at any time the velocity of *i*-th hole was proportional to the force given by Eqs. 3 and 4:

$$\frac{dx_i}{dt} = \beta F_{i,x} \tag{6}$$

$$\frac{dy_i}{dt} = \beta F_{i,y} \tag{7}$$

Eqs.3-7 describe completely motion but cannot be integrated analytically. On the other hand, they can be easily integrated numerically. We performed the task with an appropriately modified Runge-Kutta algorithm. The integration algorithm must

take into account situations when calculated displacements of the spheres lead to their overlapping, which is not allowed, of course. To prevent this, after each step of a standard Runge-Kutta integration procedure the distance between all pairs of spheres were controlled and all overlappings were immediately removed by pushing the overlapping spheres apart (along the axis determined by positions of their centres), so that they would just touch. See Fig.3. This simple procedure proved to be very effective and allowed us to simulate the particular modes of motion in which the spheres rotate in small, closely packed aggregates. The check-and-remove overlapping procedure may easily introduce unpleasant side effects like a constant drift of the controlled aggregate. One of the essential factors is the ordering in which pairs of spheres are checked. It cannot be fixed in all steps of the simulation procedure.

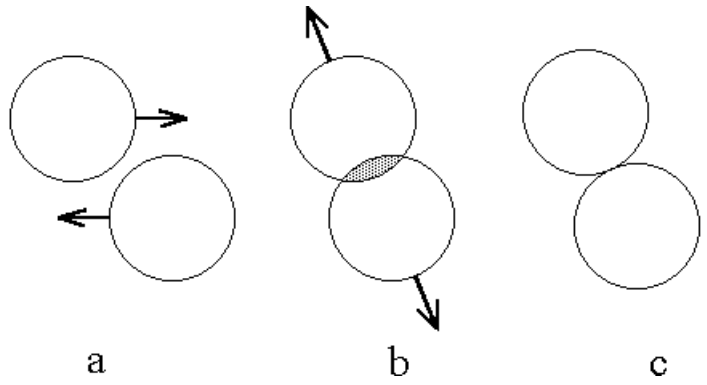

Fig.3 Scheme of the check-and-remove overlapping procedure.

a - position before the Runge-Kutta integration step. Arrows indicate directions of the calculated displacements.

b - position after the integration step. Arrows indicate directions of the remove-overlapping step.

c - final position

In what follows we put $\sigma=1$, $\alpha=1$, $H=1$ and $\beta=1$ what transforms Eqs.3-7 into a dimensionless form. The single free parameter left is thus ω - the angular velocity of the external field.

RESULTS

Below, we shall discuss a few typical modes of periodic motion observed at different frequencies of the rotating field for *N*=2,...,8.

N=2 case

In the simplest case *N*=2 motion of the pair of magnetic holes is relatively simple. For ω=0, i.e. a static magnetic field, the lowest energy configuration is achieved when the spheres stay in touch and the vector which joins their centres is parallel to the direction of the magnetic field.

As the magnetic field starts slowly rotating, the pair starts rotating as well. For a fixed ω, a constant phase lag develops. Motion of the magnetic holes is phase-locked to the motion of the magnetic field. Let us denote this mode of motion by $M_0^{(2)}$. The value of the phase lag increases with ω. See Fig.4.

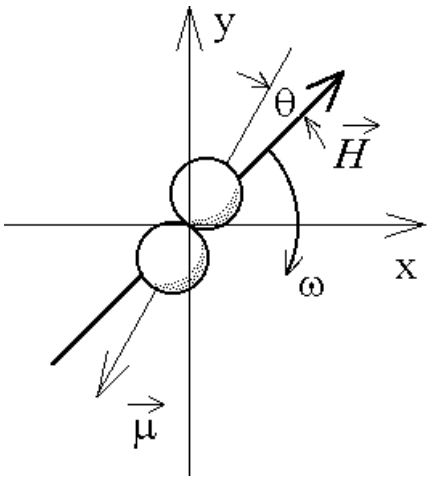

Fig.4 Configuration of the magnetic field and the pair of holes below the critical frequency $\omega_0^{(2)}$. Motion of the pair of holes is phase-locked to the motion of the magnetic field. The phase lag θ is constant with time.

At a critical value $\Omega_0^{(2)}$, the phase lag reaches its maximum $\theta =$ ($\omega_i^{(N)}, \Omega_i^{(N)}$ denote, respectively, lower and upper limits of stability for the *i*-th mode of motion observed for an aggregate of *N* magnetic holes.) As the threshold is crossed, the motion of the pair becomes more complex.

Above the maximum phase lag, the forces, which make the pair of magnetic holes follow the field, diminish. As a result, the field is able to escape and phase locked motion of the pair develops phase defects. In each of the defects the phase of the pair slips behind the field by π. During this process, the mutual orientation of the field and the pair becomes such that for a while the magnetic forces start pushing the holes apart. Thus, in addition to the jerky angular motion, a pulsing radial motion occurs. Let us denote this new mode of motion by $M_1^{(2)}$.

We come now to the problem of how to present the motion of the rotating magnetic holes. The simplest way is to show a sequence of frames cut from the numerical simulation, long enough to cover at least one period of the motion . See Fig.5.

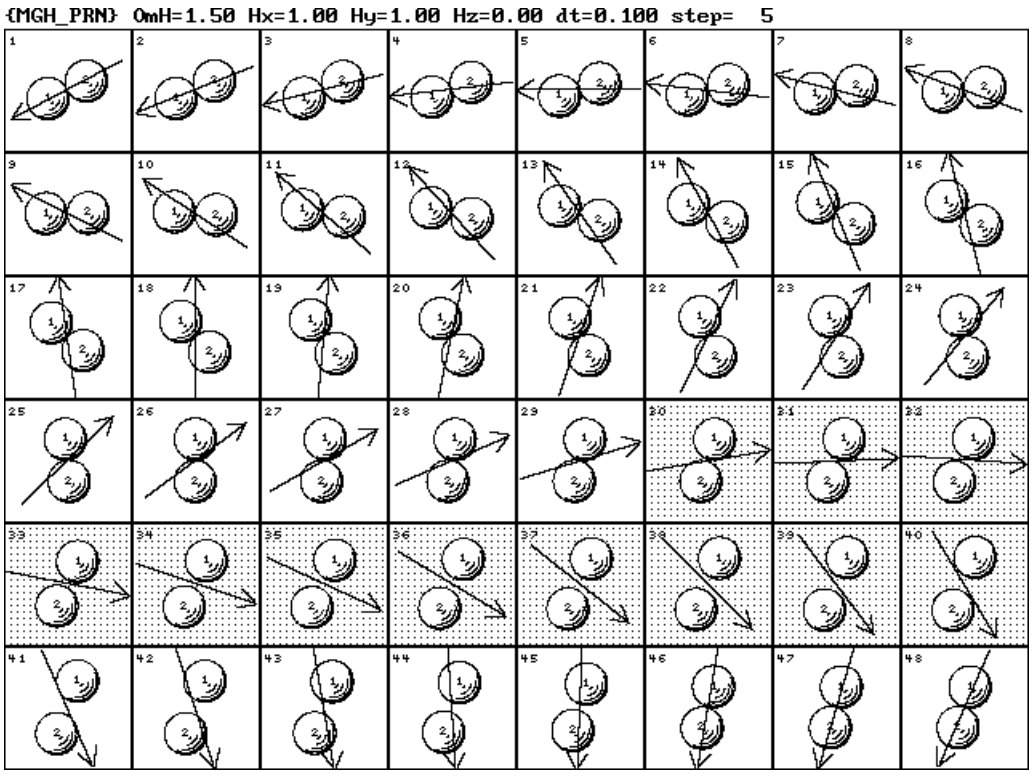

Fig.5 Motion of a pair of magnetic holes above the critical frequency $\Omega_0^{(2)}$. A phase defect in the field-pair motion is seen to develop. Frames, in which recorded configuration is such that the interaction between the spheres is repulsive are marked with a shadowed background.

In addition to the frame by frame recordings of the type shown in Fig.5 we shall apply plots in which positions of the moving spheres within the (x,y) plane (as seen at $\pi/4$ angle) are plotted versus time. To make the plots more transparent the diameter of the holes is reduced by half. As a result one may see better the internal structure of the motion. See Fig.6.

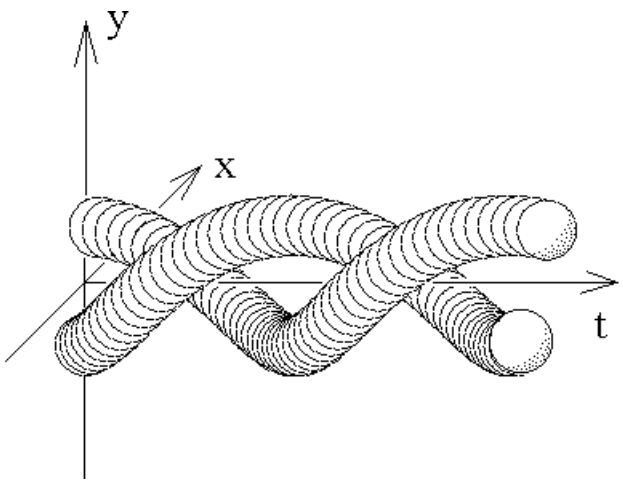

Fig.6 Structure of the space-time plots. Circular sections of the moving spheres are plotted versus time. The diameter of the spheres is reduced by half.

For the case of only two holes the plot is simple but for frequencies above the critical one it still looks rather entangled. See Fig.7

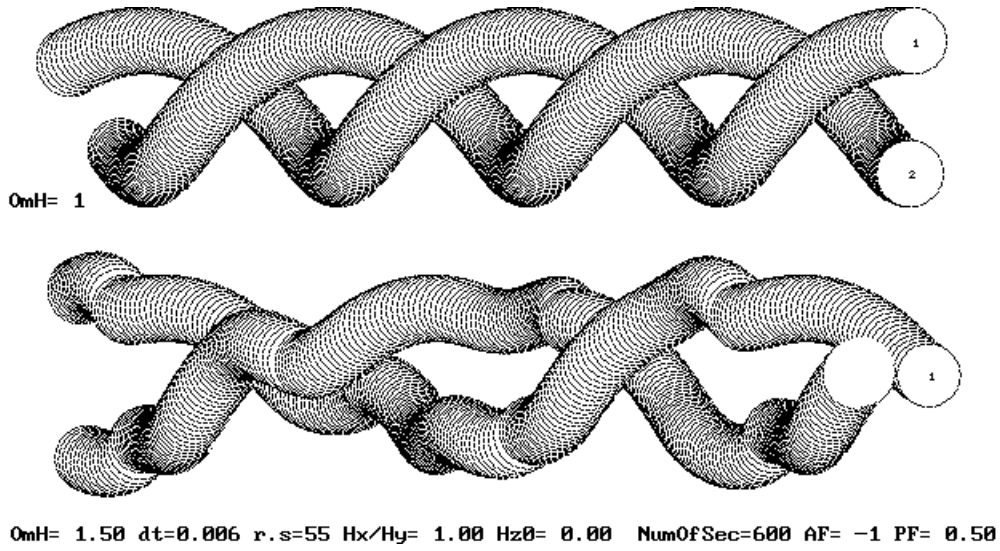

Fig.7 Space-time plot of the moving pair of magnetic holes below and above the critical frequency $\Omega_0^{(2)}$ of the rotating field as seen in the laboratory frame.

When, however, the laboratory (x,y) reference frame is changed into what we call (x', y') -"average orientation" frame, essential details of the motion become much better visible. See Fig.8.

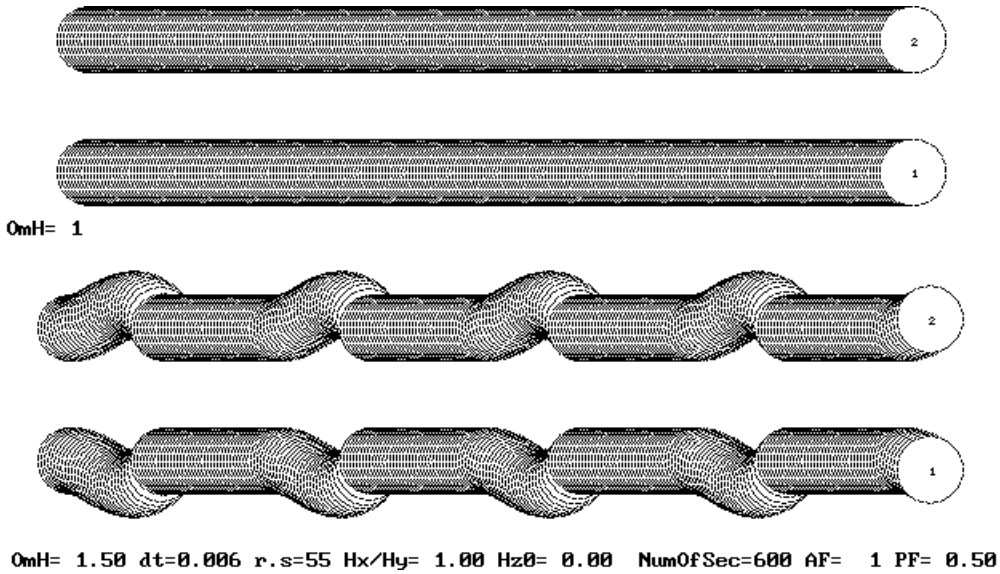

Fig.8 Space-time plot of the moving pair of magnetic holes as seen in the average direction reference frame. The pulsing radial motion of the holes above the critical frequency $\Omega_0^{(2)}$ becomes well visible.

The space-time plots of the kind shown in Fig.8 can be simplified still further. Namely, (x',y') positions of the centres of the holes can be shown but in a projection on the y' axis, which by definition determines the average orientation of the moving aggregate of holes. Since, as discussed later, such plots allow one to analyse complex periodic motions of the holes in terms of the knot theory, the traces of the centres of the holes are plotted here in form of ropes. See Fig.9.

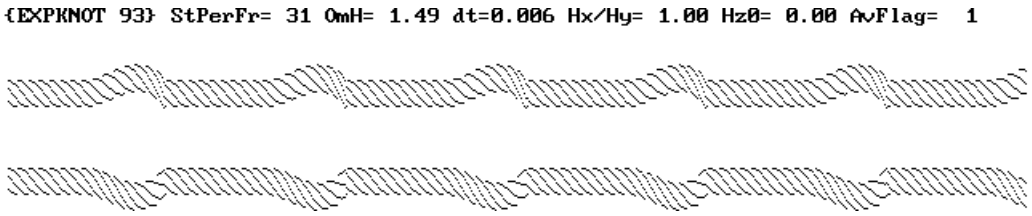

Fig.9 Y'-projected space-time plot of the motion of the centres of holes as seen in the average direction reference frame.

For increasing frequency ω of the rotating field, the average angular frequency of rotation for the pair of holes decreases. As a result, at $\omega\to\infty$ the pair ceases to rotate but stays closely packed, since the average radial force is in this case attractive.

The *N*=2 case has been considered in detail in our previous papers.[2] In particular, we studied two distinctly different versions of the case:

- two glued together spheres
- two free spheres.

The case of spheres which being glued to each other can but rotate as a couple is tractable in a rigorous analytical manner.

The case of free spheres is much more difficult from the analytical point of view. However, starting from numerical results, one is able to find some reasonable analytical approximations.

Let us mention here, that the whole problem becomes still more interesting (and difficult) when the rotating field is elliptical, i.e. its x and y components are not equal. Breaking the circular symmetry of the problem results in a few new locking type phenomena. The scope of the present study is limited but to the simpler circular case

.

N=3 case

Motion of three magnetic holes in a rotating field is quite non-trivial but once observed in a numerical simulation can be well understood in simple terms. Analysis of the problem makes a very good example of the usefulness of the numerical simulation technique.

The simplest configuration which takes place at ω=0 is easy to guess. The spheres are organised in a linear aggregate aligned in the direction of the magnetic field. As ω is small, the aggregate moves as a whole following the rotating field. Let us denote this mode of motion by $M_0^{(3)}$. See Fig.10a.

It seems worth mentioning, that in the *N*=3 case within the rotating as a whole aggregate the holes are aligned along a perfect line. As we shall see, this is not the case for *N*>3.

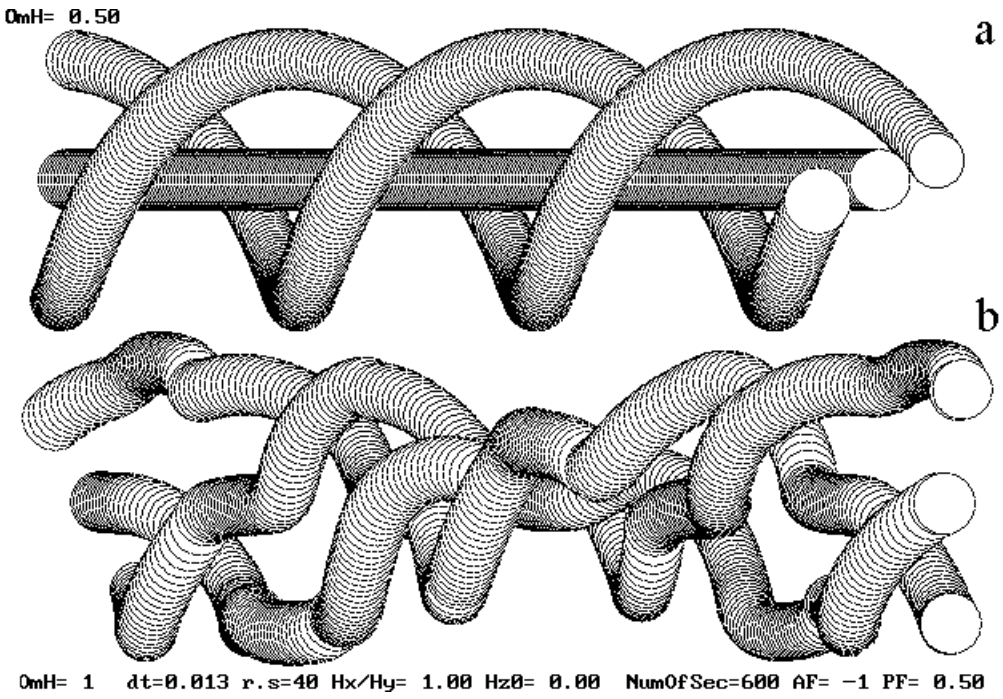

Fig.10 Space-time plot of the motion of three holes below (a) and above (b) the critical frequency $\Omega_0^{(3)}$..

Because of larger dimension of the *N*=3 linear aggregate, the steady state phase lag θ, which develops, grows faster with ω than in the *N*=2 case. Consequently,

the critical frequency $\Omega_0^{(3)}$, above which the phase-locked motion $M_0^{(3)}$ is no more possible, is smaller than in the *N*=2 case. Above the threshold a new mode of motion $M_1^{(3)}$ becomes stable. See Fig.10b.

As seen in the figure, the motion becomes more complex. Its structure is better visible in the average direction reference frame. See Fig.11.

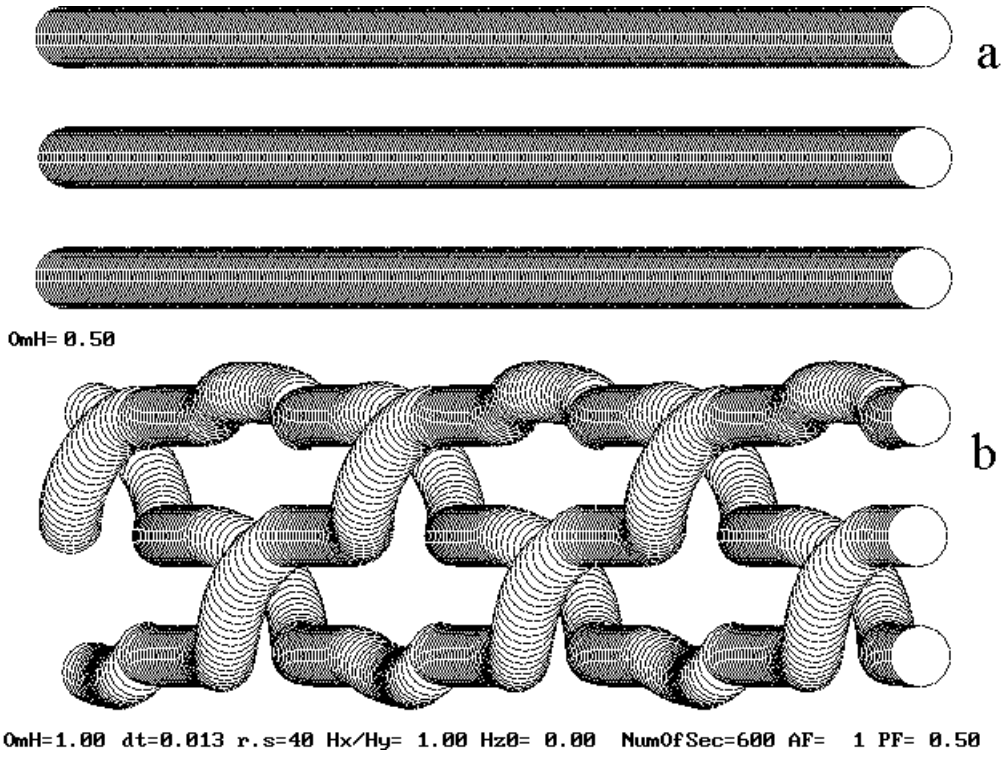

Fig.11 Space-time plot of the motion of three holes below (a) and above (b) the critical frequency $\Omega\omega_0^{(3)}$ as seen in the (*x*',*y*') reference frame.

In this reference frame, where rotation of the aggregate as a whole is removed, one can see well that in a periodic manner the aggregate is divided in two unequal parts: two of the holes remain closely packed; the third one is pushed apart. The division alternates. As a result, apart for constant phase shifts, motions of all three spheres are identical. This mode of motion remains stable up to high values of ω. See Fig.12.

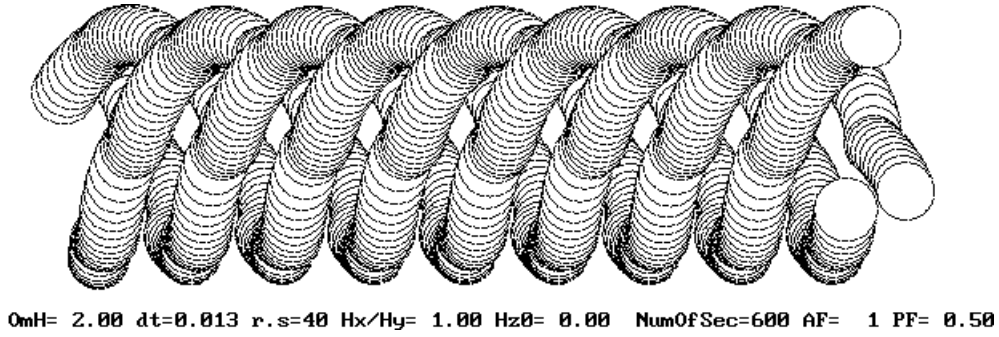

Fig.12 Same as in Fig.11. ω=2.0.

Explanation of the origin of the $M_1^{(3)}$ mode is rather interesting. Since the shape of the aggregate for frequencies below the critical one is perfectly linear, the $M_1^{(3)}$ mode must develop via a symmetry breaking. This symmetry breaking process can be observed when frequency is changed rapidly from below to above the critical one. The symmetry breaking process is well visible in the rotating average direction reference frame. See Fig.13.

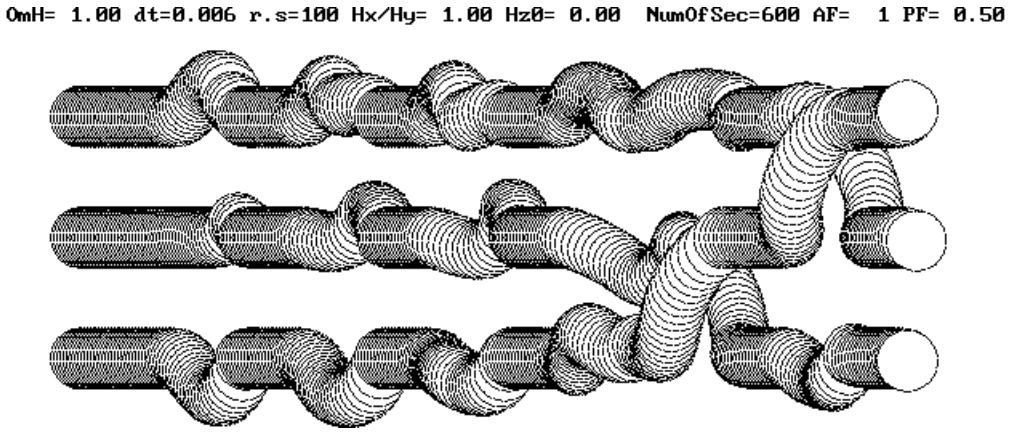

Fig.13 Symmetry breaking via which the $M_0^{(3)}$ mode turns into the $M_1^{(3)}$ mode.

While in the $M_1^{(3)}$ mode, the three holes never become collinear. This is very well visible in the sequence of frames where (x,y) positions of the spheres are plotted at discrete times .

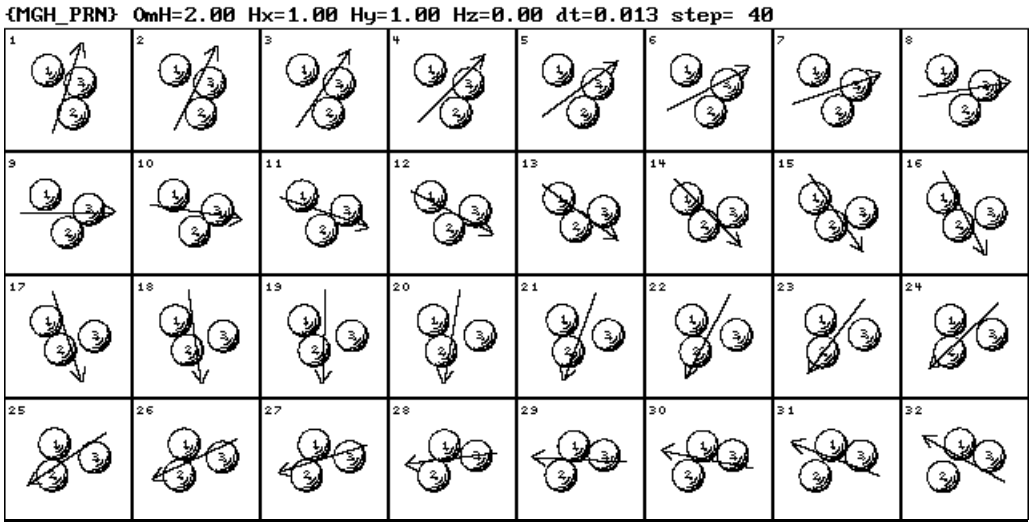

Fig.14 Sequence of frames taken from a simulation of the $M_1^{(3)}$ mode. Note that at no time the three holes become collinear. The symmetry is permanently broken.

When the frequency crosses another threshold value $\Omega_1^{(3)}$, $M_1^{(3)}$ mode collapses - the spheres become closely packed into a regular triangle.

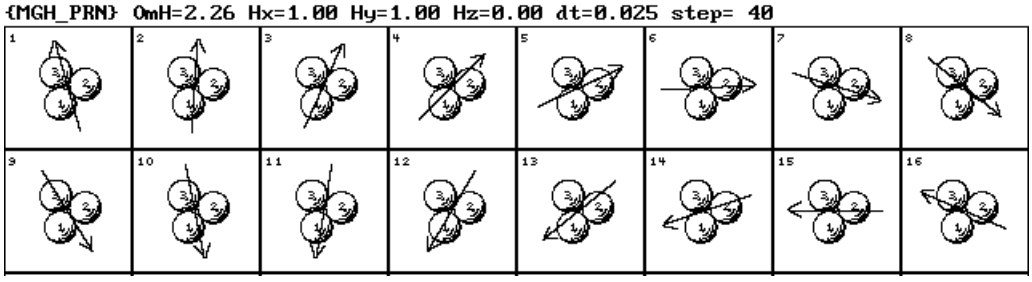

Fig.15 Above $\Omega_1^{(3)}$, $M_1^{(3)}$ mode collapses into a motionless, closely packed triangular structure.

As seen in Fig.15, due to its symmetry, the triangular aggregate does not rotate. This singular mode of (no)motion we denote by $M_3^{(3)}$. It remains stable and motionless at any frequency, also below $\Omega_1^{(3)}$. To make the holes move again, one must break the triangular configuration.

N=4 case

The set of possible modes of an aggregate of 4 magnetic holes is more rich. As previously, at small ω the linear chain rotates in phase with the magnetic field. See Fig.16.

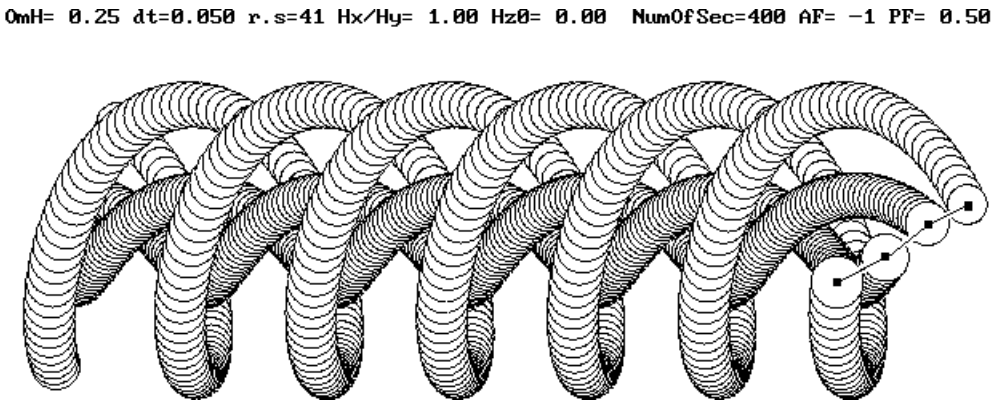

Fig.16 $M_0^{(4)}$ mode as seen in the laboratory frame. Note, that the aggregate in motion is not perfectly linear.

This phase-locked mode $M_0^{(4)}$ looses stability at the first critical frequency $\Omega_0^{(4)}$ where a new, better solution $M_1^{(4)}$ is found by the holes. See Fig.17.

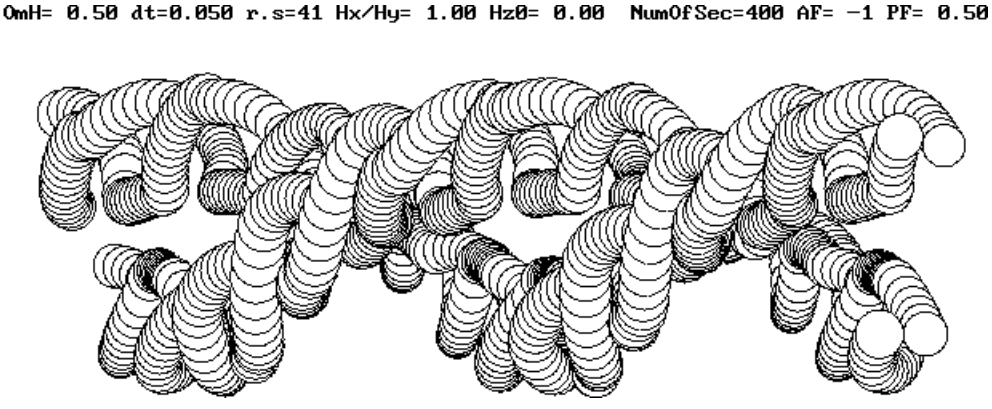

Fig.17 $M_1^{(4)}$ mode of motion as seen in the laboratory reference frame.

Its internal structure is clearly visible in the rotating reference frame (x',y').See Fig.18.

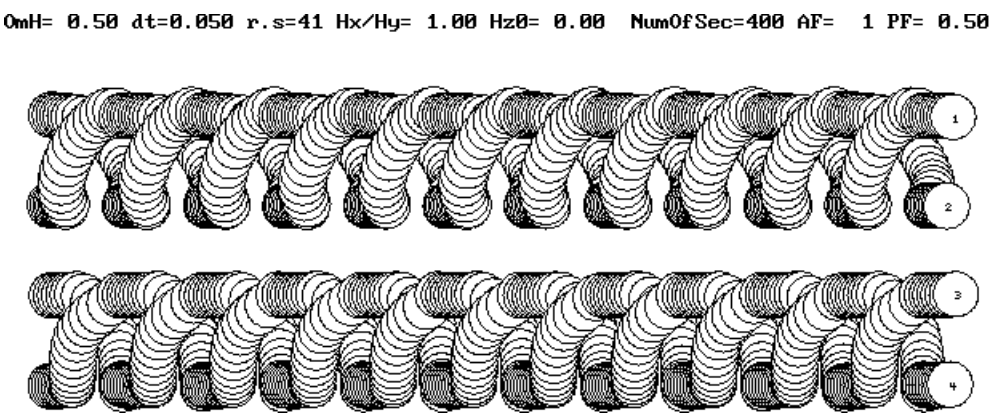

Fig.18 $M_1^{(4)}$ mode as seen in the rotating reference frame. The (x',y') average direction reference frame slowly rotates in the laboratory reference frame. See Fig.17.

Being not able to follow the rotating field as a whole linear chain, the aggregate divides periodically into two pairs, which due to their smaller dimensions are able to rotate with the frequency forced by the field. A long space-time plot taken in the laboratory frame reveals that, in addition to these partial rotations, the aggregate rotates slowly as a whole. In ballet terms, $M_1^{(4)}$ mode of motion is a waltz performed by two pairs of dancers which regularly meet to form for a while a team of four but never exchange partners. Fig.19. shows when and which of the performers touch during the dance.

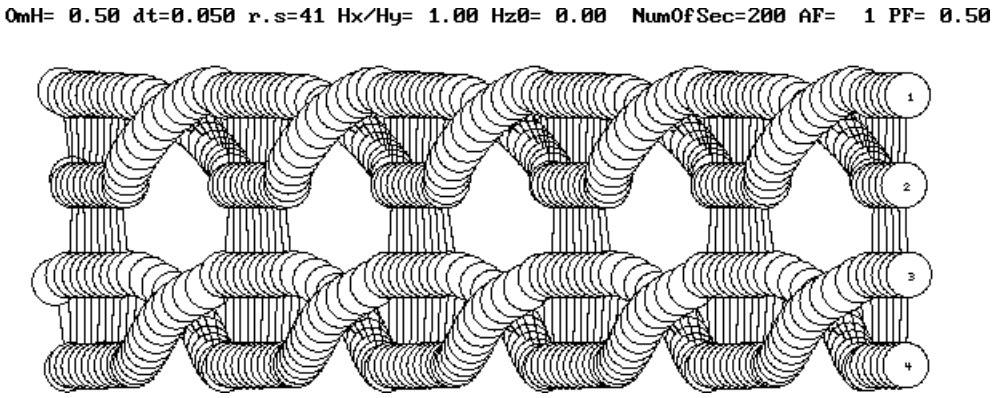

Fig.19 Space-time plot of the $M_1^{(4)}$ mode in the rotating reference frame. Lines drawn in the plot indicate which holes stay in touch a a given time.

$M_1^{(4)}$ remains stable in a broad range of frequencies from $\Omega_0^{(4)}$=0.4 to $\Omega_1^{(4)}$=1.1. In the range $\omega \in (1.1, 1.3)$ the situation is not clear. From $\omega_2^{(4)}$=1.3 up to $\Omega_2^{(4)}$=1.4 another mode of periodic motion - $M_2^{(4)}$ is observed. See Fig.20.

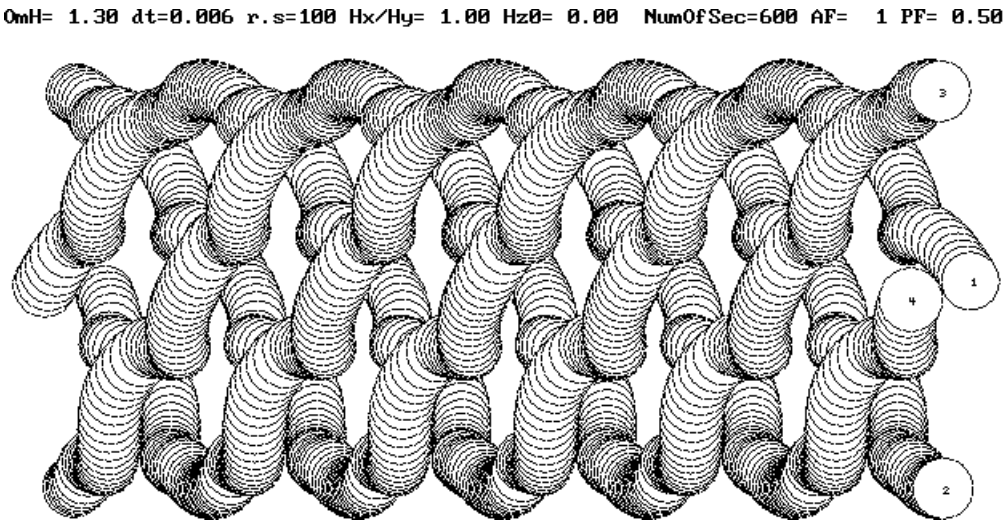

Fig.20 $M_2^{(4)}$ as seen in the (x',y') reference frame. Compare with Fig.17.

The magnetic hole dance presented in the figure is no more a simple waltz performed by two pairs of dancers. Here, after each turn, the pairs exchange those partners which are at the time inside the group. As a result of this "turn in pairs, change partners" rule, each performer dances for a while with any other. The rule is better seen within a sequence of frames. See Fig.21 and 22. Note the numbers which index the dancers.

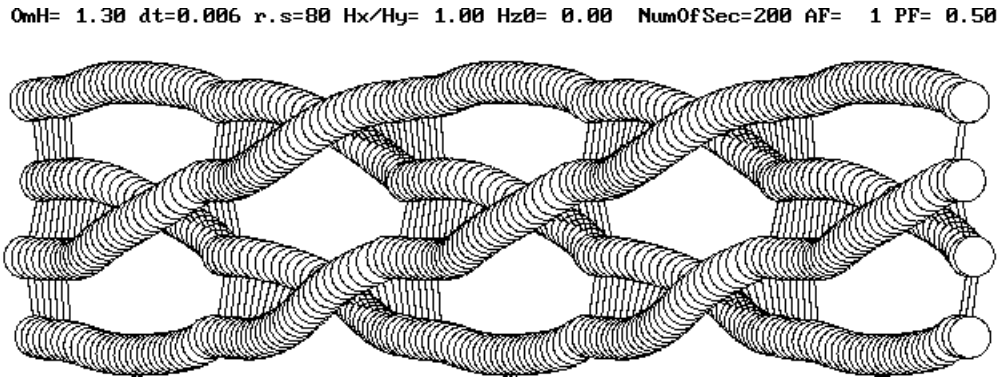

Fig. 21 $M_2^{(4)}$ mode of motion as seen in the rotating reference frame. Bonds drawn in the figure indicate when and which of the holes stay in touch at a given moment of time.

Fig.22 Sequence of frames taken from simulation of the $M_2^{(4)}$ mode of motion as seen in the laboratory reference frame.

Above $\Omega_2^{(4)}$=1.35 $M_2^{(4)}$ mode collapses. The holes become packed into a compact, slightly oscillating parallelepiped. This new, compact form of motion denoted by $M_3^{(4)}$ is stable up to infinite frequencies. On the other hand $M_3^{(4)}$ proves to be stable also below the threshold at which it was born. However, when ω drops below $\omega_3^{(4)}=\Omega_4^{(4)}$=0.95, its oscillations turn into what can be described as a "breathing' mode - $M_4^{(4)}$. See Fig.23.

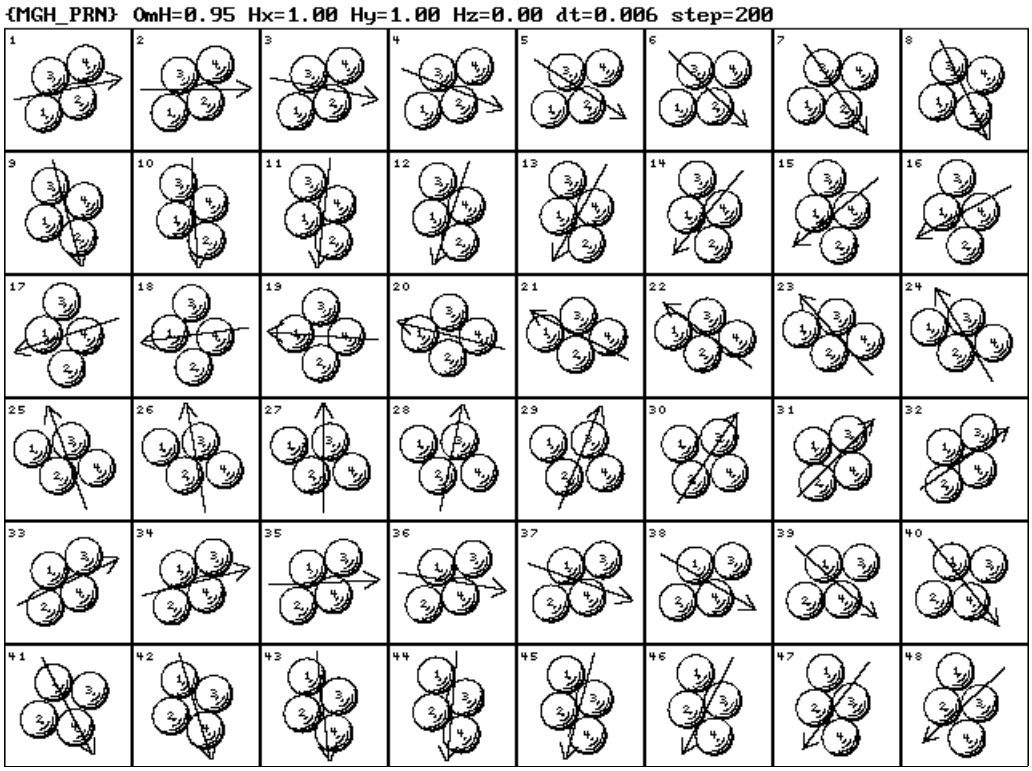

Fig.23 The breathing mode of the compact form of the aggregate of four magnetic holes.

Below $\omega_4^{(4)}=0.53$ the breathing mode looses stability and the aggregate recovers its linear form. Experiments described above prove that at a given value of ω a few stationary modes of motion may be possible. Which of the modes is chosen depends on the history of the system, or, from a different point of view, on the initial conditions. This is a typical feature of nonlinear systems.

N=5 case

Motion of five magnetic holes is still more rich. As previously, we start with the phase locked mode $M_1^{(5)}$, whose range of stability covers frequencies from $\omega_1^{(5)}$=0 to $\Omega_1^{(5)}$=$\omega_2^{(5)}$=0.24 above which a new $M_2^{(5)}$ mode becomes stable.

. At $\omega_1^{(5)}$=0 the chain of holes is perfectly linear. As ω increases its shape is distorted into an S-shaped curve. See Fig.24. This distortion is observed for any *N*>3. Certainly, there should be a neat analytical approximation for it, at least for large *N*.

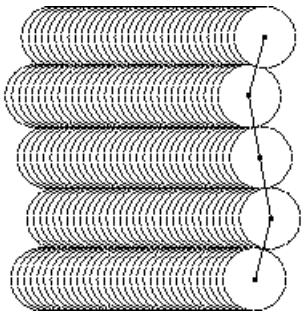

.

Fig.24 The S-shape of the rotating chain of magnetic holes observed within the $M_1^{(5)}$ mode of motion close to its upper stability limit $\Omega_1^{(5)}$. ω=0.23. The space-time plot is made in the rotating (x',y') reference frame. Magnetic holes are plotted at their full diameter.

Above the threshold the linear aggregate of five magnetic holes is not able to follow the field as a whole and is forced to divide into smaller pieces. Due to the odd number of holes there is a confusion how to divide the chain. Solution of the problem is identical to that we already discussed at *N*=3 case. The most democratic division, 2-1-2, would conserve symmetry of the S-shape observed for the $M_1^{(5)}$ mode, but proves to be unstable. In such a division the central hole should stay all time at the origin of the reference frame, at which the symmetry axis is located, while the 2 hole pieces would individually catch up and follow the field. As easy to see, this is not a local minimum of the magnetic energy for the whole interval of the rotation of the 2 hole pieces. Consequently, the symmetry is broken and the aggregate becomes

divided into two unequal pieces, of 2 and 3 holes, which due to their small linear dimensions are able to catch up and follow the field. After a rotation by π, the two pieces unite into a single aggregate, but its shape is no more a symmetrical *S*. For a while the aggregate rotates as a single, connected piece. During this time its shape evolves slightly. In the next crisis the division has the same structure. This mode of motion we denote by $M_2^{(5)}$. See Fig.25.

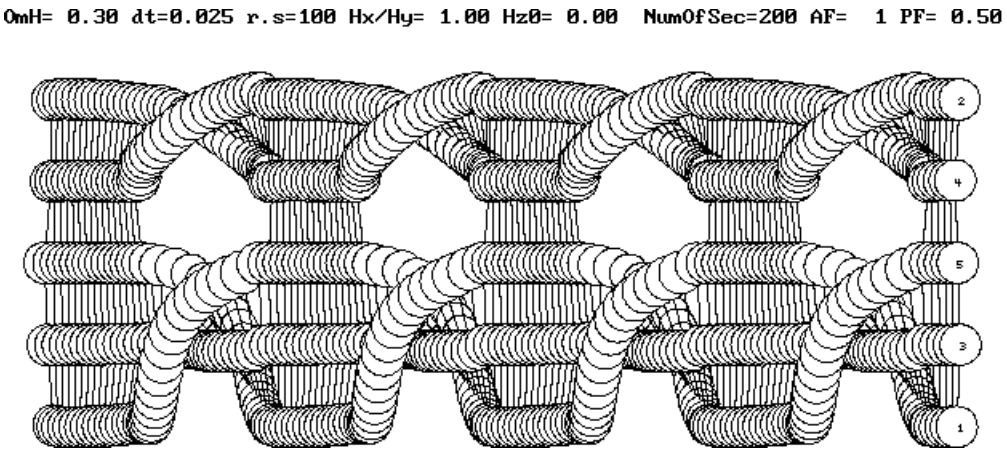

Fig.25 $M_2^{(5)}$ mode as seen in the rotating reference frame. Spheres which stay in contact are connected with linear bonds.

Above $\Omega_2^{(5)}$=0.37 the $M_2^{(5)}$ mode looses stability and gives place to a new mode - $M_3^{(5)}$. See Fig.26. In this mode the division into a couple and a triple of holes alternates.

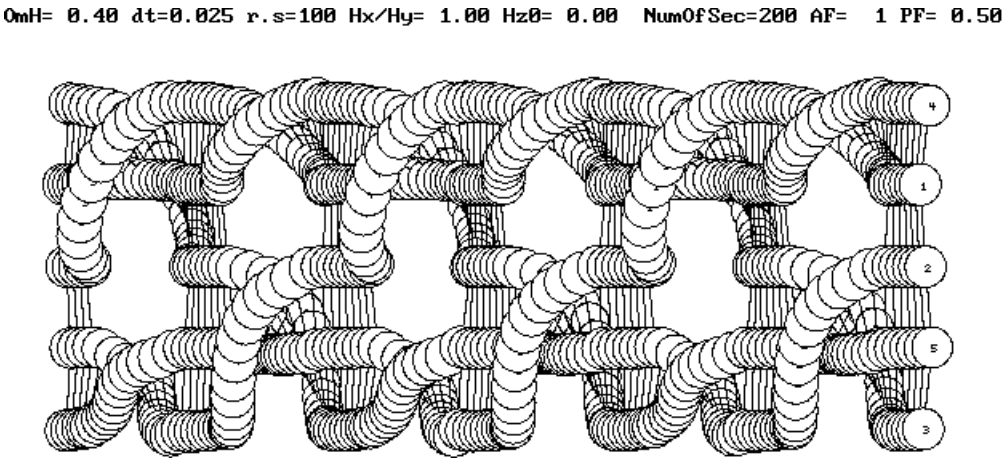

Fig.26 $M_3^{(5)}$ mode as seen in the rotating reference frame. Spheres which stay in contact are connected with lines.

Mode $M_2^{(5)}$ can be seen as a composition of one $M_0^{(2)}$ and one $M_0^{(3)}$ mode. The modes are strongly coupled but, as seen in Fig.25, although deformed, they preserve their identity. This interaction changes with ω what at ω=0.37 makes them to mix. The resulting motion is rather complex and sensitive to parameters of the integration procedure, thus we would not like to draw at the moment too firm conclusions. What seems, however, certain is that at ω=0.4 the $M_3^{(5)}$ mode settles down. In this mode, as seen in Fig.26, the mixing process becomes regular. The $M_3^{(5)}$ proves to be stable up to $\Omega_3^{(5)}$=0.9. Close to the threshold the mechanism of the motion becomes clear. Frame by frame recordings reveal it. See Fig.27.

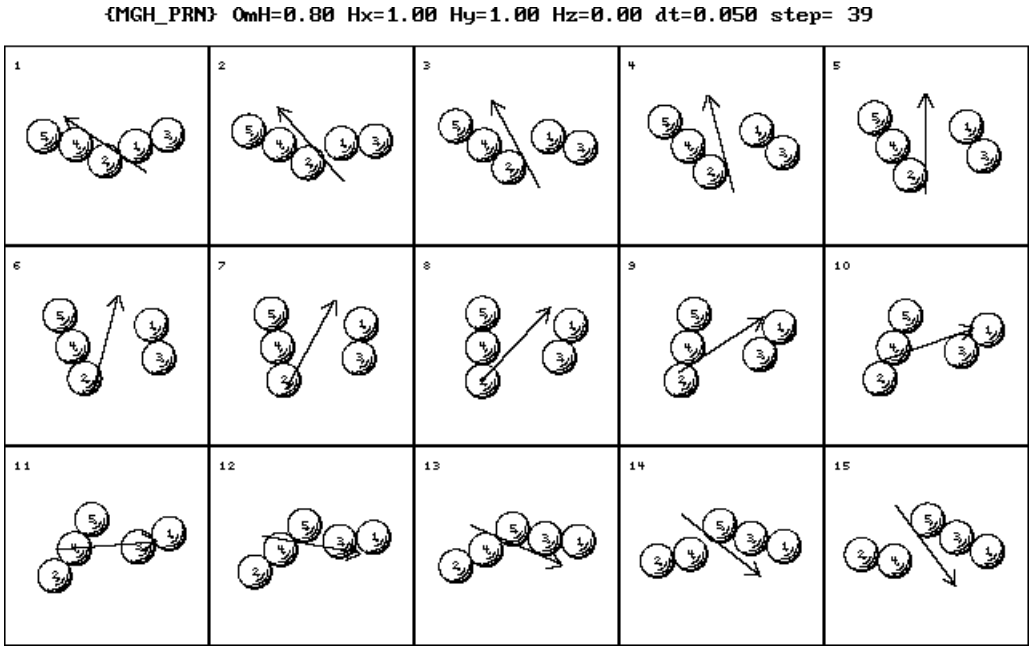

Fig.27 A few frames recorded during simulation of the $M_3^{(5)}$ mode. Note the V-shaped form of the aggregate and the position of the magnetic field at the moments when all holes stay in touch.

Being longer, the three hole piece has more problems to follow the field. The V-shaped form of the aggregate makes it easier. Namely the aggregate is always cut in such a manner that the direction of the three hole piece stays closer to the field that of the two hole piece.

In the frequency range form 1.0 up to 1.2 the situation is not clear. We have not identified any type of a periodic motion. We cannot state, however that the motion in this region is chaotic. Problems of the type remain open.

Above $\omega_4^{(5)}$=1.3 a new, very interesting mode of periodic motion $M_4^{(5)}$ becomes stable. Fig.28 presents a piece of the space-time plot of it.

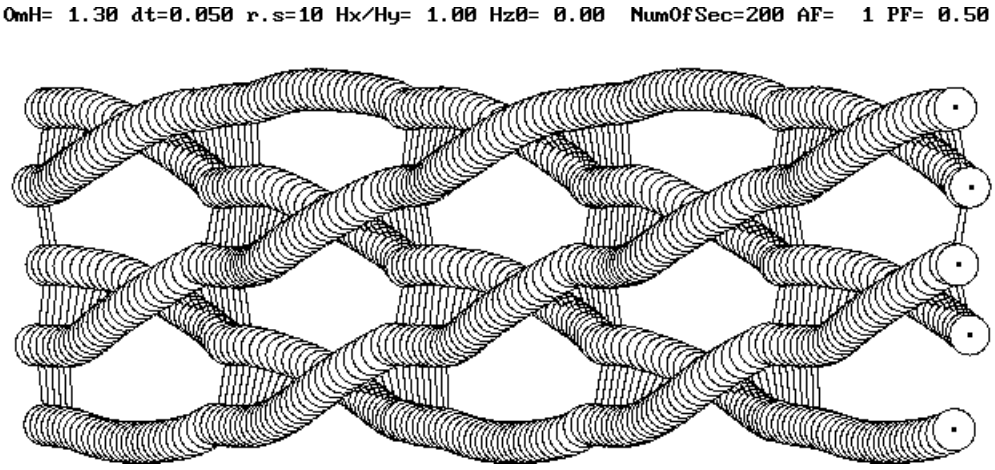

Fig.28 $M_4^{(5)}$ mode of motion as seen in the rotating (x;'y') reference frame.

Here the aggregate of five holes is cut by the rotating field into three pieces: two pairs and a single. The single is always located at the ends of the aggregate. The frame by frame recording shows it even better. Fig.29.

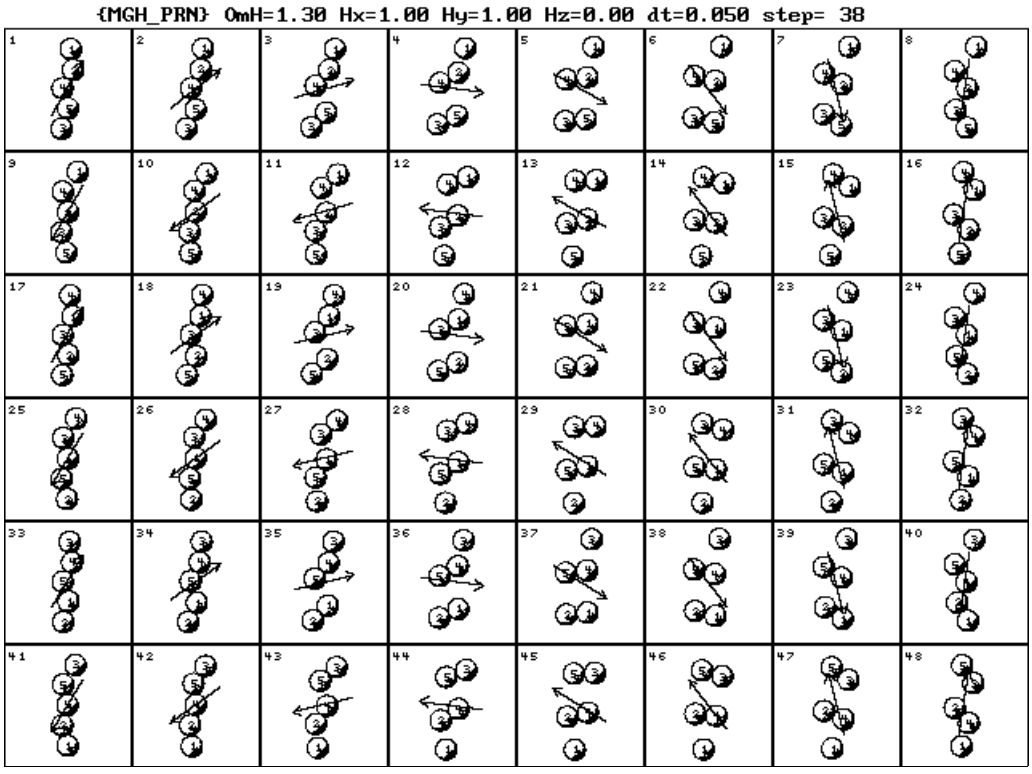

Fig.29 Frame by frame story of the hole motion while within the $M_4^{(5)}$ mode.

The time distance at which consecutive frames were recorded was chosen such that one "unit cell" of the motion covers one row of the table of frames.

The $M_4^{(5)}$ mode remains stable up to $\Omega_4^{(5)}$=1.43. Above the threshold it collapses and a compact aggregate is formed. As in the *N*=4 case it oscillates slightly. The oscillating mode of motion we denote by $M_5^{(5)}$. See Fig.30.

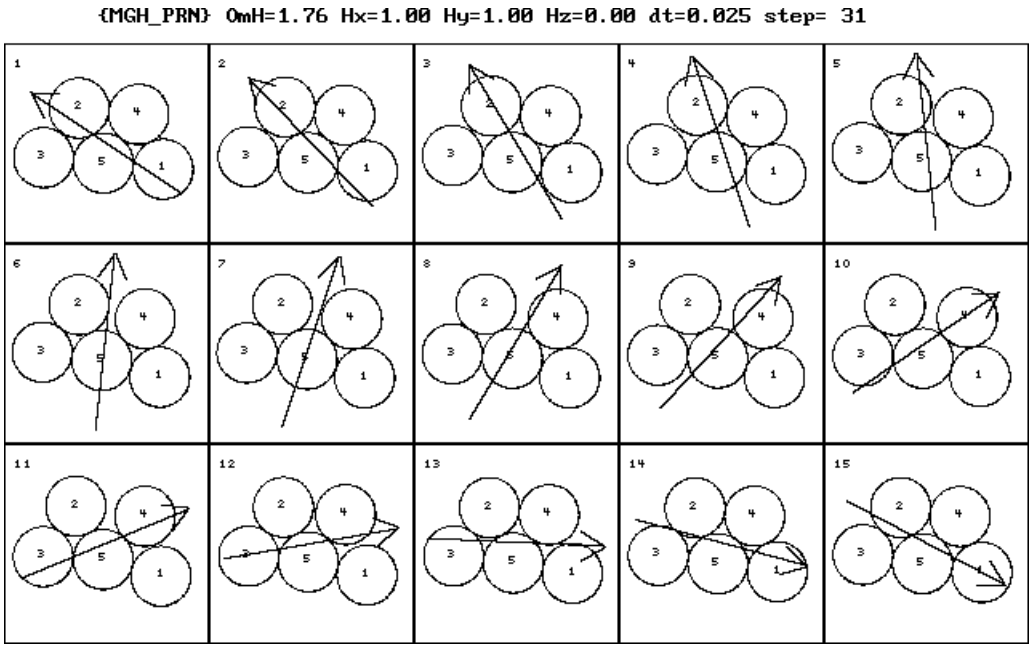

Fig.30 One period of the oscillation of the compact aggregate of five holes formed above $\Omega_4^{(5)}$=1.43.

The compact form of the aggregate remains stable also for lower frequencies. At ω=0 it is closely packed; this is just another low energy configuration of five holes. For ω small enough, ω<$\Omega_6^{(5)}$=0.25, the aggregate rotates as a whole following the field. We denote this mode of motion by $M_6^{(5)}$

.

N=6 case.

The *N*=6 case is the last we present. Collection of its mode of motion starts with a single chain phase-locked mode $M_0^{(6)}$. The S-shaped deformation of the linear configuration is still better visible here.

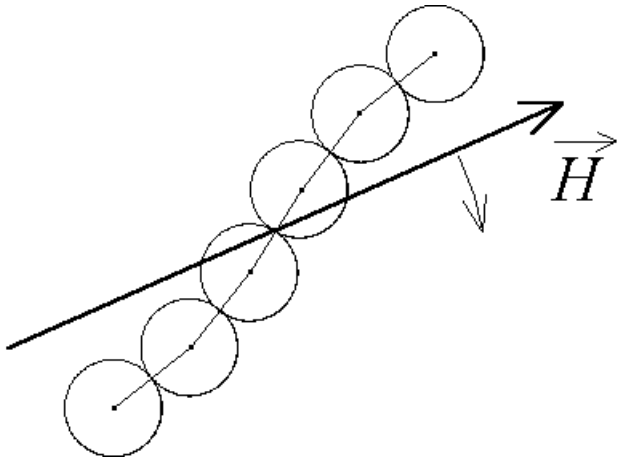

Fig. 31 The S- shaped deformation of a single chain aggregate of 6 magnetic holes close to the upper stability limit of the $M_0^{(6)}$ mode. ω=0.15.

The $M_0^{(6)}$ mode looses stability above $\Omega_0^{(6)}$. Above the threshold the phase lag crosses its critical value and the chain is forced to find a different way of following the escaping field. The solution is obvious: it divides into two equal pieces, which being shorter are able to follow the field. This mode of motion analogous to all previously discussed $M_1^{(N)}$ modes, where *N* is an even number. We present it here in form of a rope type plot. See Fig.32.

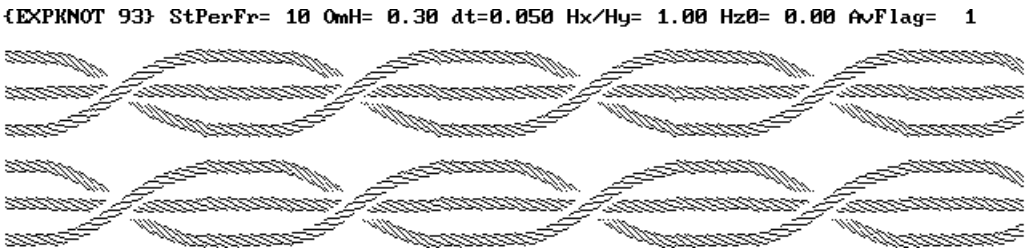

Fig.32 Rope representation of the $M_1^{(6)}$ mode. The plot is made in the rotating reference frame.

The divide-in-two-and-rotate solution proves to be too slow above $\Omega_1^{(6)}$=0.5 threshold. The obvious alternative is divide-in-three-and-rotate. Indeed, this kind of motion, let us denote it by $M_3^{(6)}$, is observed in the frequency range from $\omega_3^{(6)}$=0.6 to $\Omega_3^{(6)}$=0.8. See Fig.34. In-between, another, intermediate solution $M_2^{(6)}$ is found. See Fig.33.

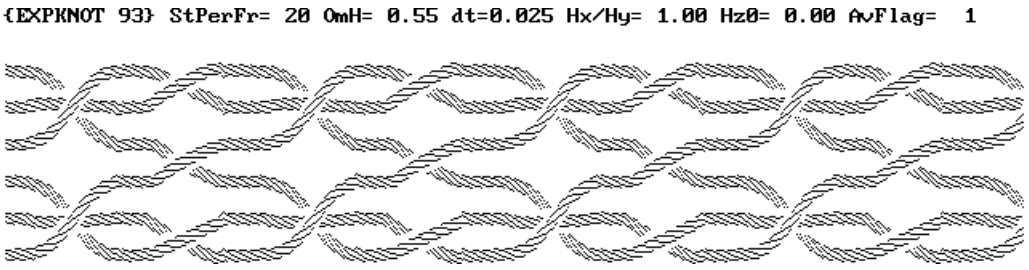

Fig.33 Rope representation of the $M_2^{(6)}$ mode

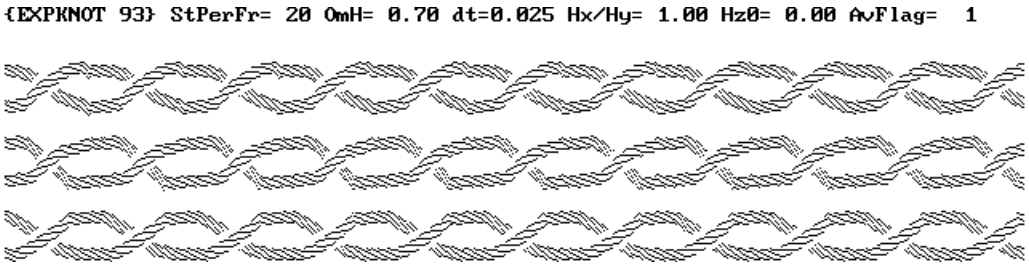

Fig.34 Rope representation of the $M_3^{(6)}$ mode

The $M_3^{(6)}$ mode proves to be stable in a narrow frequency range. Its precise determination needs some more work. Anyway, it is unstable for $\omega \in (0.9, 1.2)$ we

have not found any kind of a periodic motion. However, at $\omega = 1.3$ motion of the 6 holes once more proves to be periodic. See Fig.35.

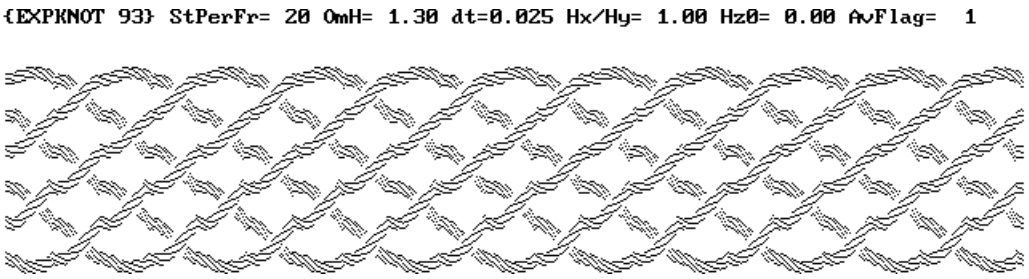

Fig.35 Rope representation of the $M_4^{(6)}$ mode.

THE PROBLEM OF PERIODICITY

Rotational motion of magnetic holes seems to be very interesting from the formal point of view. The basic questions one asks solving numerically equations of motion are:

(i) Is the motion periodic?

(ii) If so, which is its period?

First of all, let us note that what matters here is not the laboratory frame configuration of the holes $\{x_i(t), y_i(t)\}_{i=1}^N$, which should repeat itself after a certain time *T*,

$$\{x_i(t+kT), y_i(t+kT)\}_{i=1}^N = \{x_i(t), y_i(t)\}_{i=1}^N, \quad \text{k=1,2,...} \tag{8}$$

but rather their configuration as seen within the reference frame rotating with the magnetic field: $\{x_i''(t), y_i''(t)\}_{i=1}^N$. All forces which make the system move depend on the relative positions of the holes and the magnetic field. The motion is periodic if this relative configuration is recovered in equal intervals of time:

$$\left\{x_i''(t+kT), y_i''(t+kT)\right\}_{i=1}^{N} = \left\{x_i''(t), y''(t)\right\}_{i=1}^{N}, \text{ k=1,2,...} \qquad (9)$$

For the sake of clarity, most figures we presented were plotted in the "average direction" reference frame (x',y'). Let us explain in more detail how the position of the reference frame was determined all calculations.

Centres of N holes in question make in the laboratory (x,y) plane a kind of discrete plot which in a standard manner one can fit with a straight line. (In the case when at ω=0 the holes are arranged in a linear chain the lines just goes through the centres of the holes.) Except for some singular configuration the straight line fit is well defined. The average direction reference frame thus defined rotates with the aggregate.

Using the notion of the average direction reference frame one can define periodic motion as such in which:

$$\left\{x_i'(t+kT), y_i^{©}(t+kT)'\right\}_{i=1}^{N} = \left\{x_i'(t), y_{i'}'(t)\right\}_{i=1}^{N}, \text{ k=1,2,...} \qquad (10)$$

Let us note that when the motion as seen in the (x',y') reference frame repeats itself with periodicity T so must repeat itself the phase the phase of the magnetic field as seen in the same reference frame

$$\varphi_H'(t+kT) = \varphi_{H'}'(t) \qquad (11)$$

Definition of periodicity given by Eq. 10 is too restrictive. It requires that all magnetic holes recover their original positions within the rotating aggregate. Analysing figures we presented one can easily notice that each of the plots of periodic motions is composed from units which are much shorter. Definition of the periodicity must take into account the fact that even when the holes do not return to their original positions, the overall shape of the aggregate can be recovered. Thus, the proper definition should be as follows:

Definition

Motion of N magnetic holes is periodic when

$$\left\{x'_{p(i)}(t+kT_p), y'_{p(i)}(t+kT_p)\right\}_{i=1}^{N} = \left\{x'_i(t), y'_i(t)\right\}_{i=1}^{N}, \quad k=1,2,... \qquad (12)$$

where p(i), i=1, 2, ..., N, denotes an arbitrary permutation of the indexes which number the holes.

The shortest interval of time T_p *for which Eq.12 is fulfilled is called the* ***permutational period*** *of motion.*

HOLES AND KNOTS

Plots of the magnetic holes motion as seen in the average direction reference frame invite one to apply basic notions of the knot theory. Interpreting the space-time trajectories of the holes as ropes one may ask what kind of knots one obtains connecting ends of a few period segment of such trajectories to their beginnings.

To start with let us analyse a few simplest cases. For *N*=2, there is but one answer. Both for the $M_0^{(2)}$ and $M_1^{(2)}$ modes , regardless the length of the trajectory segment the ends joining procedure leads to two disconnected loops. See Fig.36.

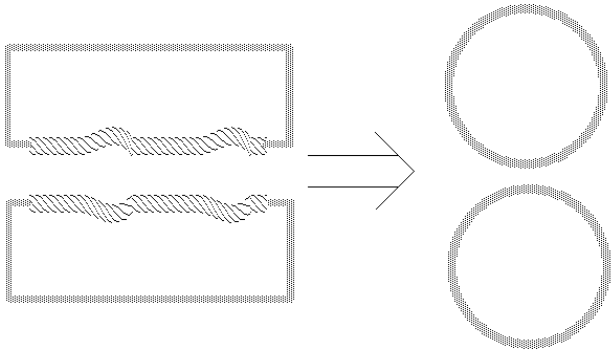

Fig.36 Knot analysis of the $M_1^{(2)}$ mode.

Situation is much different for *N*=3. Here, results of the ends joining procedure depend on both the mode studied and the length of the trajectory segment.

Within the $M_0^{(3)}$ mode trajectories of the all three particles never mix. As a result the knot scheme is analogous to that of $M_0^{(2)}$ and $M_1^{(2)}$ modes.

Within the $M_1^{(3)}$ mode the trajectories change places. Knot scheme depends on the length of the segment. See Fig.37.

If the length of the segment is equal to the permutational period T_p of the mode, its knot scheme is equivalent to a single loop.

If the length of the segment is equal to $2T_p$ then its knot scheme is equivalent to the trefoil knot.

Finally, if the length is equal to $3T_p$ then the knot scheme of the segment is equivalent to the Borromean Rings.

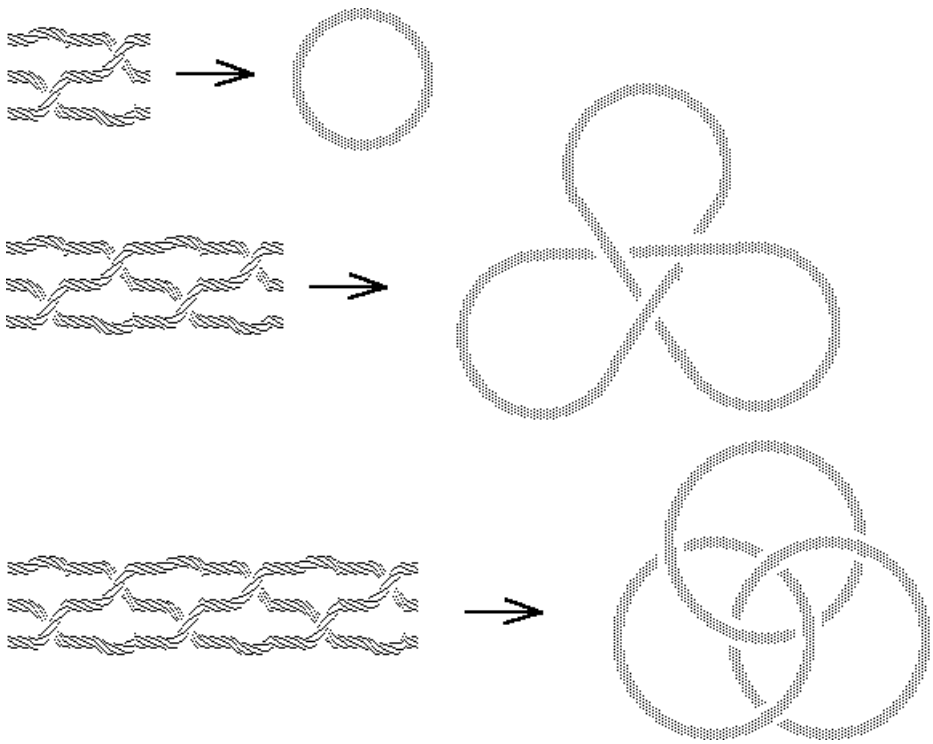

Fig.37 Knot analysis of the $M_1^{(3)}$ mode.

..... to be continued.

REFERENCES

[1]A. T. Skjeltorp, Phys. Rev Lett. **51**, 2306 (1983)

A. T. Skjeltorp, J. Magn. Mat. **65**, 195 (1987)

[2]G. Helgesen, P. Pierañski and A. T. Skjeltorp, Phys. Rev. Lett. **64**, 1425 (1990)

G. Helgesen, P. Pierañski and A. T. Skjeltorp, Phys. Rev. **A42**, 7271 (1990)